ISSN 1070-3284, Russian Journal of Coordination Chemistry, 2022, Vol. 48, No. 4, pp. 242–249. © Pleiades Publishing, Ltd., 2022.
Russian Text © The Author(s), 2022, published in Koordinatsionnaya Khimiya, 2022, Vol. 48, No. 4, pp. 248–256.

Synthesis, Structure and Magnetic Properties of New Ionic Ni–Yb Nitrate Complexes with 2,2'-Bipyridine and 1,10-Phenanthroline

P. N. Vasilyev[a], *, A. V. Gavrikov[a], A. B. Ilyukhin[a], and N. N. Efimov[a]

[a] *Kurnakov Institute of General and Inorganic Chemistry RAS, Moscow, Russia*

**e-mail: anubisvas@gmail.com*

Received August 30, 2021; revised October 14, 2021; accepted October 18, 2021

Abstract—New heterometallic nitrate complexes, namely $[Ni(bipy)_3][Yb(NO_3)_5]\cdot 0.58MeOH$ (**I**), $[Ni(phen)_3][Yb(NO_3)_5]$ (**II**) and $[Ni(phen)_3][Yb(NO_3)_5]\cdot MeOH$ (**II**·MeOH), have been prepared and studied. Anions $[Yb(NO_3)_5]^{2-}$ in these complexes are the first examples of homoleptic ten-coordinatied Yb complexes. The magnetic behavior of single-phase **I** and **II** has been studied in static and dynamic modes. A field-induced slowdown of magnetic relaxation, i.e., properties of single-ion magnets (SIMs), was revealed for **I** and **II**. Thus, **I** and **II** are rare examples of 3*d*–4*f*-coordination compounds possessing a discrete structure rather than a joint metal core and demonstrating a slowdown in the relaxation of magnetization. The interplay between the properties of SIM and structural features of **I** and **II** was established (CIF CCDC files no. 2103796 (**I**), 2103797 (**II**), 2103798 (**II**·MeOH)).

Keywords: heterometallic 3*d*–4*f*-complexes, nickel(II), ytterbium(III), single-ion magnets, magnetostructural correlations

DOI: 10.1134/S1070328422040066

INTRODUCTION

Currently, heterometallic 3*d*–4*f* coordination compounds (CCs) are among the most intensively studied groups of complexes due to a range of interesting, and even unique properties, e.g. magnetic [1–6], luminescent [7–9], etc. In turn, the most prominent direction in the study of the magnetic properties of such CCs is the search for new efficient single-molecule magnets (SMMs), i.e. complexes exhibiting a significant slowdown of the relaxation of magnetization after turning off the external magnetic field [10, 11]. Thus, such CCs can be considered as a potentially more efficient alternative to common magnetic materials for the information recording, processing and storage [12–16].

One of the main stimuli for the search for new 3*d*–4*f*-SMMs is the opportunity to slow the magnetic relaxation by suppressing quantum tunneling of magnetization (QTM). It becomes possible due to the significant magnetic interactions between 3*d*- and 4*f*-metal centers [17, 18]. The latter, in turn, inspires studies of oligo- and polynuclear systems with small (3–4 Å) distances between metal centers joint by various bridging ligands [19, 20]. At the same time, heterometallic CCs, the structures of which are formed by discrete mononuclear complexes, still remain practically unexplored.

It should also be noted that studies of 3*d*–4*f*-SMM are mainly focused on systems comprising Kramers ions of heavy lanthanides, i.e. those with an odd number of *f*-electrons [21, 22]. In turn, the majority of corresponding studies deal with Dy-containing complexes [23–26], while complexes formed by other Ln^{3+} have been studied in much less detail [8]. This is due to the well known bistability of the ground electronic state of Dy^{3+} which persists regardless of the symmetry of the ligand field [27]. As a result, the requirements for the geometry of the coordination environment (CE) to enhance intrinsic magnetic anisotropy are significantly less strict in the case of Dy^{3+} and its complexes. Heterometallic SMMs based on other Ln^{3+} are still much less studied [8].

Herein, we report first results of studying non-disprosium 3*d*–4*f* complexes formed by discrete metal centers and exhibiting SMM/SIM properties. In particular, new ionic Ni–Yb complexes—$[Ni(bipy)_3][Yb(NO_3)_5]\cdot 0.58MeOH$ (**I**), $[Ni(phen)_3][Yb(NO_3)_5]$ (**II**) and $[Ni(phen)_3][Yb(NO_3)_5]\cdot MeOH$ (**II**·MeOH) were prepared and studied using hydrated metal nitates and bidentate N-donor ligands 2,2'-bipyridine (bipy) and 1,10-phenanthroline (phen). The compounds were characterized by single-crystal XRD and powder XRD, elemental analysis and IR spectroscopy. The magnetic behavior of single-phase samples **I** and **II** was studied in static and dynamic modes, i.e. under static and alternating magnetic fields.

EXPERIMENTAL

The following commercial reagents and solvents were used for the synthesis: $Ni(NO_3)_2 \cdot 6H_2O$ (reagent-grade; Khimmed) and $Yb(NO_3)_3 \cdot 5H_2O$ (99.99%; Lanhit); 2,2'-bipyridine, bipy (99+%, Alfa Aesar); monohydrate of 1,10-phenanthroline, phen·H_2O (99%, Sigma-Aldrich), methyl alcohol CH_3OH (extra pure grade; Khimmed). All chemicals were used as received.

Synthesis of $[Ni(bipy)_3][Yb(NO_3)_5] \cdot 0.58MeOH$ (I). To the solution of $Ni(NO_3)_2 \cdot 6H_2O$ (0.125 g, 0.43 mmol) in 30 mL of hot (64°C) MeOH, bipy (0.201 g, 1.29 mmol) was added, and the mixture was stirred at 64°C for 5 min. The color of the solution changed from turquoise to red-pink. Then $Yb(NO_3)_3 \cdot 5H_2O$ (0.193 g, 0.43 mmol) was added and the mixture was stirred at 64°C for 5 min. After the evaporation of the resulting solution at 64°C under reduced pressure (water-jet pump), pink-red crystalline product containing crystals suitable for structural studies (single-crystal XRD) was formed. According to powder XRD (Fig. S1), this product was single phase **I**. The yield was 0.269 g (61%).

For $C_{30.58}H_{26.32}N_{11}O_{15.58}NiYb$ (M = 1028.93)

Anal. calcd., %	C, 35.66	H, 2.56	N, 14.97
Found, %	C, 35.11	H, 2.08	N, 14.49

ATR-IR of **I** (ν, cm^{-1}): 3308 (w), 3107 (w), 3080 (w), 2944 (vw), 2834 (w), 1780 (w), 1732 (w), 1602 (m), 1576 (w), 1569 (m), 1480 (s), 1470 (vs), 1439 (s), 1310 (vs), 1246 (m), 1225 (m), 1173 (m), 1156 (m), 1122 (w), 1105 (m), 1071 (w), 1065 (w), 1044 (w), 1027 (s), 1023 (s), 972 (w), 912 (w), 890 (w), 813 (m), 756 (s), 749 (s), 735 (s), 653 (m), 633 (m), 582 (w), 571 (w), 548 (w), 530 (w), 500 (w), 479 (w), 467 (w), 445 (w), 418 (m).

In the case of **$[Ni(Phen)_3][Yb(NO_3)_5]$ (II)**, the preparation and evaporation of the solution was carried out similarly using Phen·H_2O (0.255 g, 1.29 mmol) instead of bipy. Powder XRD (Fig. S2) as well as single crystal XRD examination of several crystals of the isolated product showed that this product is a mixture of **II** and $[Ni(Phen)_3][Yb(NO_3)_5] \cdot MeOH$ (**II**·MeOH). After the 3 h exposition of this product at 70°C, 0.275 g (59%) of single-phase **II** (Fig. S3) was obtained.

For $C_{36}H_{24}N_{11}NiO_{15}Yb$ (M = 1082.4)

Anal. calcd., %	C, 39.95	H, 2.24	N, 14.24
Found, %	C, 39.71	H, 1.97	N, 14.01

ATR-IR of **II** (ν, cm^{-1}): 3317 (w), 3110 (w), 3078 (w), 2945 (vw), 2832 (w), 1779 (w), 1734 (w), 1600 (m), 1577 (w), 1570 (m), 1480 (s), 1470 (vs), 1439 (s), 1418 (m), 1311 (vs), 1246 (m), 1223 (m), 1174 (m), 1158 (m), 1121 (w), 1106 (m), 1071 (w), 1065 (w), 1044 (w), 1027 (s), 1023 (s), 972 (w), 912 (w), 890 (w), 813 (m), 753 (s), 750 (s), 738 (s), 656 (m), 630 (m), 582 (w), 573 (w), 548 (w), 530 (w), 502 (w), 478 (w), 467 (w), 447 (w), 420 (m).

Single crystal X-ray diffraction (single crystal XRD). The experimental data sets for complexes **I**, **II**, and **II**·MeOH were obtained on a Bruker SMART APEX2 diffractometer equipped with a CCD camera and a MoK_α radiation source with a graphite monochromator [28]. Absorption was taken into account by the semiempirical method for equivalents (SADABS) [29]. The structures were solved by a combination of the direct method and Fourier syntheses. The H atoms are positioned from geometric considerations. The occupancies of disordered atoms were obtained by isotropic refinement with fixed U_{iso} = 0.03 Å^2 for disordered atoms and were set as constant in further calculations. The structures were refined by full-matrix anisotropic least squares fitting, the H atoms were taken into account in the riding model. All calculations were performed using the SHELXS and SHELXL programs [30]. Crystallographic data and the refinement statistics are given in Table 1.

The experimental parameters for the investigated structures were deposited at the Cambridge Crystallographic Data Center (CCDC nos. 2103796 (**I**), 2103797 (**II**), 2103798 (**II**·MeOH); deposit@ccdc.cam.ac.uk; http://www.ccdc.cam.ac.uk).

Powder X-ray diffraction study (powder XRD) was carried out on a Bruker D8 Advance diffractometer (CuK_α, Ni-filter, LYNXEYE detector, reflection geometry).

Elemental C,H,N analysis was carried out according to standard methods on a EUROEA 3000 CHN analyzer.

Infrared spectra were recorded in the attenuated total internal reflection mode (ATR-IR) in 400–4000 cm^{-1} range using a Bruker ALPHA instrument equipped with a diamond tool.

Magnetic measurements. The magnetic susceptibility measurements were carried out using a Quantum Design PPMS-9 automated complex for physical measurements with an option for measuring magnetic properties. This device allows measuring magnetic properties in the 1.8–300 K temperature range under an external magnetic fields up to 9 T. Dynamic magnetic susceptibility measurements were performed at an alternating magnetic field with a strength of 1, 3, and 5 Oe in the frequency ranges of 10000–1000, 1000–100, and 100–10 Hz, respectively. These settings allow both to avoid heating the sample at low temperatures (which can occur at high amplitudes and modulation frequencies), and to obtain the best signal-to-noise ratio. The measurements were carried out on polycrystalline samples covered with mineral oil and sealed in polyethylene bags in order to prevent

Table 1. Crystal data and structure refinement for **I**, **II**, **II**·MeOH

Parameter	Value		
	I	**II**	**II**·MeOH
Empirical formula	$C_{30.58}H_{26.32}N_{11}O_{15.58}Ni$	$C_{36}H_{24}N_{11}O_{15}NiYb$	$C_{37}H_{28}N_{11}O_{16}NiYb$
Formula weight	1028.93	1082.41	1114.46
Temperature, K	150(2)	120(2)	150(2)
Radiation (λ, Å)	MoK_α (0.71073)	MoK_α (0.71073)	MoK_α (0.71073)
Crystal system	Triclinic	Monoclinic	Triclinic
Space group	$P\bar{1}$	$P2_1/n$	$P\bar{1}$
a, Å	9.3215(2)	17.6752(4)	10.8817(4)
b, Å	12.8645(3)	12.4625(3)	11.8947(4)
c, Å	16.2933(3)	19.2690(4)	16.6488(6)
α, deg	81.6190(10)	90	92.0658(13)
β, deg	78.2550(10)	110.7970(10)	106.2592(12)
γ, deg	76.7270(10)	90	102.1921(13)
V, Å^3	1851.75(7)	3967.96(16)	2011.65(12)
Z	2	4	2
ρ(calc.), g/cm^3	1.845	1.812	1.840
μ, mm^{-1}	3.106	2.903	2.868
F(000)	1019	2140	1106
Crystal size, mm	0.32 × 0.24 × 0.10	0.28 × 0.2 × 0.10	0.2 × 0.18 × 0.12
θ Range, deg	2.181–33.068	2.116–33.089	2.280–27.485
Index ranges h, k, l	$-14 \le h \le 14$, $-19 \le k \le 18$, $-24 \le l \le 24$	$-26 \le h \le 25$, $-19 \le k \le 19$, $-28 \le l \le 29$	$-14 \le h \le 14$, $-15 \le k \le 15$, $-21 \le l \le 21$
Reflections collected	28427	59840	30320
Independent reflections (R_{int})	12673 (0.0234)	14032 (0.0418)	9171 (0.0297)
Completeness to θ = 25.242°, %	100.0	99.9	99.7
Max, min transmission	0.2693, 0.1737	0.7465, 0.488	0.7461, 0.6108
Data/restraints/parameters	12673/72/630	14032/54/629	9171/2/627
Goodness-of-fit	0.990	1.022	0.989
R_1, wR_2 ($I > 2\sigma(I)$)	0.0255, 0.0657	0.0276, 0.0611	0.0238, 0.0431
R_1, wR_2 (all data)	0.0304, 0.0682	0.0384, 0.0652	0.0277, 0.0447
$\Delta\rho_{max}/\Delta\rho_{min}$, e/Å^3	0.887/–0.652	1.429/–0.741	0.770/–0.527

the field-induced orientation of crystallites. The paramagnetic component of the magnetic susceptibility (χ) was determined taking into account the diamagnetic contribution of the sample, estimated by the additive Pascal formula, as well as the contributions of the sample holder and mineral oil.

RESULTS AND DISCUSSION

New complexes **I** and **II** have been prepared by the interaction of Ni and Yb nitrates with the common bidentate N-donor ligands bipy and phen in methanolic solutions. Noteworthy, while virtually monophasic **I** crystallize from bipy-containing solutions, the primary product isolated from phen-containing systems is always a mixture of solvent-free and solvated complexes, **II** and **II**·MeOH. A similar situation was previously observed for ionic Sm–Co nitrate complexes [31].

Despite the simplicity of the compositions and similar structural motif of the $[M(Q)_3][Ln(NO_3)_5(L')_x]\cdot y$Solv complexes formed in $M(NO_3)_2\cdot 6H_2O$–$Ln(NO_3)_3\cdot xH_2O$–Q–Solv systems (M = Co, Ni; Q = bipy and phen; Solv = solvents), it is rather difficult to obtain single-phase samples of these complexes. This

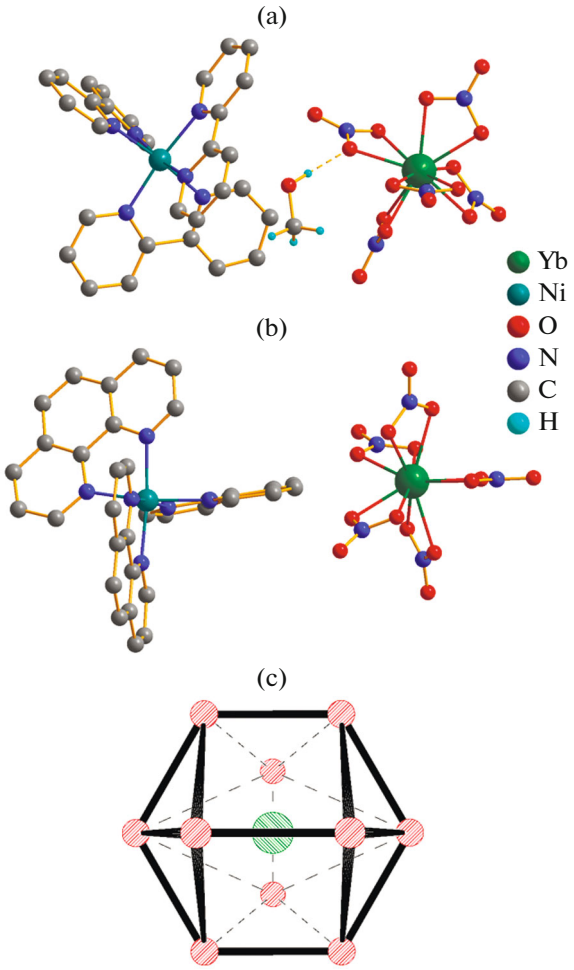

Fig. 1. Molecular structures of **I** (a) and **II** (b) and ideal tetradecahedral geometry (c). H atoms of bipy and phen molecules are omitted for clarity.

is due to the alternating qualitative and quantitative compositions of the L' ligands and lattice Solv molecules. The most common L' ligands are molecules of coordinating solvents such as water [31–33] and light alcohols [31, 34, 35]. Thus, even when absolute solvents are used for the synthesis, there is considerable probability to isolate a mixture of products of similar composition rather than monophasic $[M(Q)_3][Ln(NO_3)_5(L')_x]\cdot y$Solv species.

However, coordination with L' ligands is more preferable in systems containing cations of light lanthanides such as La^{3+} [32–35] and Sm^{3+} [31]. This is obviously due to the rather large ionic radii of such cations. In Yb-containing systems, such processes virtually do not occur since the ionic radius of Yb^{3+} is notably smaller, because of the lanthanide contraction [36]. Indeed, there are no reported CCs with $[Yb(NO_3)_5(L')_x]$ moieties (CSD, version 5.42, May 2021). This allows us to conclude that the structural diversity of $[M(Q)_3][Ln(NO_3)_5(L')_x]\cdot y$Solv complexes for Ln = Yb is mainly determined by the qualitative and quantitative composition of lattice Solv molecules.

Compound **I** is isostructural to the reported $[Co(bipy)_3][Sm(NO_3)_5]\cdot 0.61$MeOH complex [31]. Structure of **I** is formed by mononuclear complex cations $[Ni(bipy)_3]^{2+}$ and $[Yb(NO_3)_5]^{2-}$ anions (Fig. 1a), as well as lattice MeOH molecules. The occupancy of the MeOH site is ~1/2. The reproducibility of this result was confirmed by X-ray diffraction analysis of single crystals of **I** obtained in the repeated synthesis. These crystals were taken under a layer of mother liquor, then mounted directly in the mother liquor on a holder under perfluorinated oil protection and placed under a current of cold N_2 (T = 100 K). In the $[Yb(NO_3)_5]^{2-}$ structure, the Yb atom is coordinated by ten O atoms of five chelating NO_3^-, four NO_3^- are disordered.

Complexes **II** and **II**·MeOH are formed by complex cations $[Ni(Phen)_3]^{2+}$ and $[Yb(NO_3)_5]^{2-}$ anions (Fig. 1b, S4). In the case of **II**·MeOH, there are also lattice MeOH molecules. Three and two of five NO_3^- ligands are disordered in the anionic complexes in **II** and **II**·MeOH, respectively.

The Ni atoms in the cationic complexes **I**, **II**, and **II**·MeOH have the usual octahedral environment. The structure of the anionic complexes $[Yb(NO_3)_5]^{2-}$ in compounds **I** and **II**, **II**·MeOH is different. In structure of **I**, there is significant rotation of two positions of disordered NO_3^- towards each other (the O...O distances of the two positions reach 1.40 Å). In structures **II** and **II**·MeOH, the rotation of the two positions of disordered NO_3^- ligands towards each other is significantly smaller—the O...O distances of the two positions are 0.74 Å (**II**) and 0.76 Å (**II**·MeOH).

Despite this difference, the geometry of the coordination polyhedron (CP) of Yb atom in all three CCs is similar, and, according to SHAPE calculations [37], is closest to the tetradecahedron (Fig. 1c, Table S1).

If NO_3^- ligands are considered as "normalized bites" [38], then these ligands form a trigonal-bipyramidal environment around the Yb atom. In Fig. 1c, it is clearly seen that two axial NO^{3-} are below and above the plane, while three equatorial NO^{3-} form the plane of the figure.

Noteworthy, the survey of the known structures of Yb-containing CCs (CSD, version 5.42, May 2021) revealed almost complete absence of complexes (both homo- and heterometallic) containing ten-coordinated Yb^{3+} in absolutely homoleptic coordination environment. This allows us to conclude that the compounds studied in this work are the first representatives of such CCs.

The magnetic behavior of monophasic **I** and **II** was studied by the static (direct-current, dc) and dynamic

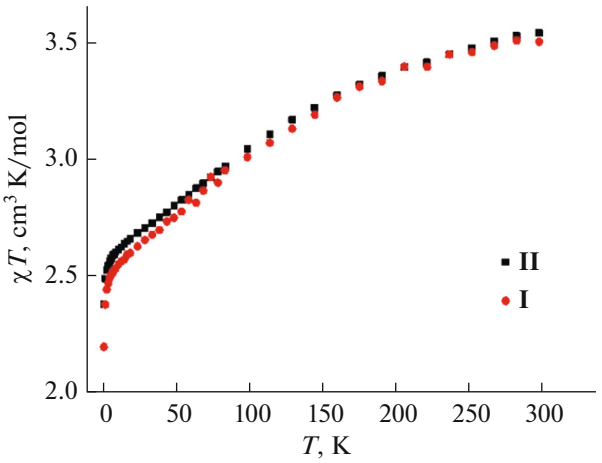

Fig. 2. χT vs. T dependencies for **I** and **II** under static magnetic field of 5000 Oe.

(alternating current, ac) magnetic susceptibility. The study in a static mode was carried out in the range of 2–300 K under the static magnetic field of 5000 Oe. The form of the obtained χT dependences (Fig. 2) is determined by the contribution of both Yb^{3+} and Ni^{2+}. The χT value at 300 K is 3.56 and 3.54 $cm^3\ mol^{-1}\ K$ for **I** and **II**, respectively. These values are close to the sum of the theoretical values for non-interacting Yb^{3+} ($S = 1/2$, L = 3, $g = 8/7$, $^2F_{7/2}$, $\chi T = 2.57\ cm^3\ mol^{-1}\ K$) and Ni^{2+} ($S = 1$, $^3F_4$, $g_{Ni} = 2.20$, $\chi T = 1.01\ cm^3\ mol^{-1}\ K$) [39]. Upon the decrease in temperature, the χT values monotonically decrease to 20 K, then a sharper decrease to the minimal values at $T = 2$ K (2.2 and 2.4 $cm^3\ mol^{-1}\ K$ for **I** and **II**, respectively) occurs. Such behavior may be due to the spin–orbit interaction, the thermal depopulation of Stark sublevels of Yb^{3+}, the zero-field splitting of the m_J levels caused by the ligand field and/or the Zeeman (saturation) effect [40]. The contribution of the Ni^{2+}–Yb^{3+} exchange interactions, which are usually notable for the known Ni–Yb complexes [41, 42] with joint metal core, can be neglected in the case of **I** and **II**. This is due to the discreteness of **I** and **II** structures together with large distances between the metal centers. The shortest distances between metal centers in structures **I** and **II** are given below:

Compound	Yb...Yb, Å	Ni...Ni, Å	Yb...Ni, Å
I	8.94, 9.27	8.74, 9.32	7.02, 7.03
II	9.48, 9.67	9.57, 9.63	6.89, 7.75

In order to establish whether **I** and **II** are SIMs, i.e. exhibit slowdown of magnetic relaxation, the magnetic behavior of **I** and **II** in the ac mode (in alternating magnetic fields) was studied. For both complexes, no significant signal is observed on the frequency dependences of the imaginary component of the

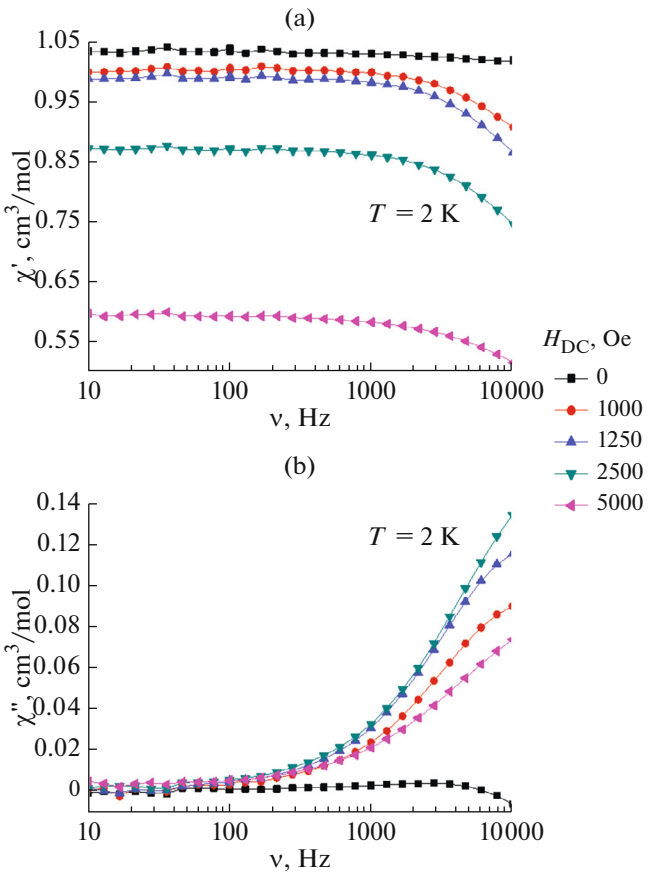

Fig. 3. Frequency dependencies of real, χ' (a), and imaginary, χ'' (b), components of magnetic susceptibility of **I** under various applied magnetic fields at 2 K. Solid lines are visual guides.

dynamic magnetic susceptibility obtained under zero magnetic field (Figs. 3, 4), i.e. there is no slow magnetic relaxation under these conditions. Such situation is typical for Yb^{3+} CCs [43–49], and is most likely due to the contribution of the quantum tunneling of magnetization (QTM) [50], which accelerates the relaxation of magnetization.

Application of static magnetic fields of various strengths made it possible to observe non-zero values of the imaginary component of the dynamic magnetic susceptibility for **I** and **II** (Figs. 3b, 4b). However, the absence of clear-cut maxima in all the dependences within the operating range of the applied equipment (10–10000 Hz) does not allow one to determine the quantitative characteristics of the relaxation of magnetization for both complexes. This result clearly shows that considerable contribution of the QTM mechanism to the relaxation of magnetization in **I** and **II** remain significant in the entire range of applied static fields.

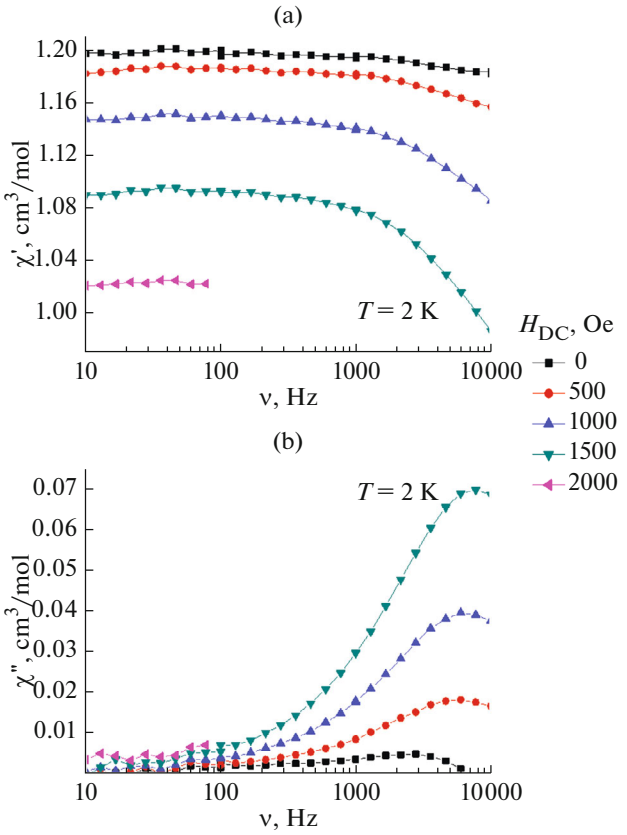

Fig. 4. Frequency dependencies of real, χ' (a), and imaginary, χ" (b), components of magnetic susceptibility of **II** under various applied magnetic fields at 2 K. Solid lines are visual guides.

The magnetic behavior of heterometallic Ni–Yb CCs is still relatively poorly studied [40–42, 51]. In addition, almost all known studies concern systems with joint metal core, i.e. with metal centers connected by various bridging ligands and located relatively close (3–4 Å) to each other. Therefore, exchange and/or dipole-dipole magnetic interactions have a significant effect on the magnetic behavior of such systems. On the contrary, structures **I** and **II** are formed by discrete and distant mononuclear complexes (see above). This allows assuming the decisive role of the CE configuration of isolated Yb^{3+}on the magnetic behavior of **I** and **II** in the dynamic mode.

In [52], the geometries of the CE, which are the most optimal for maximizing the magnetic anisotropy (and, therefore, the properties of SMM/SIM) of particular Ln^{3+} were theoretically predicted. According to this model, the most optimal CE for the Yb^{3+} ion possessing an elongated configuration of electron density is CE with equatorial symmetry, i.e. with donor centers of ligands forming an equatorial plane. This conclusion is confirmed by the known reports of homometallic ytterbium SMM. Indeed, the largest known energy barrier to magnetization reversal is exhibited by nine-coordination $[N(C_2H_5)_4]_3[Yb(Dipic)_3]\cdot nH_2O$ complex (Dipic = dianion of pyridine-2,6-dicarboxylic acid) with tricapped trigonal prismatic Yb^{3+} CE [54] where "capping" donor centers form a slightly distorted equatorial plane.

From the point of view of the model proposed in [52], unimpressive SMM properties of **I** and **II** rise from:

(1) the presence of apical NO_3^- in the CE of Yb^{3+} (Figs. 5a, 5c). It prevents the enhancement of the intrinsic anisotropy of Yb^{3+}.

(2) strong distortion of the equatorial plane in comparison with the ideal tetradecahedral CE (Figs. 5b, 5c).

The third possible factor influencing the nature of the relaxation of remanent magnetization in **I** and **II** is the qualitative composition of Yb^{3+} CE. Previously, the negative effect of the homoleptic CE on SIM performance of Yb-based CCs regardless of its geometry was revealed by thorough literature survey of mononuclear complexes [47]. However, this assumption still requires further experimental verification since the scarcity of SMMs/SIMs formed by Yb^{3+}.

Thus, new Ni–Yb heterometallic nitrates have obtained and studied. Unlike the vast majority of the known heterometallic CCs of these metals, the structures of the compounds are formed by mononuclear complex ions rather than oligo- or polynuclear heterometallic complexes with metal ions joint by bridging ligands. Anions $[Yb(NO_3)_5]^{2-}$ in the obtained CCs are examples of practically unknown homoleptic ten-coordination Yb complexes. Measurements of the dynamic magnetic susceptibility of the obtained CCs showed that the relaxation of the magnetization occurs too quickly even under external magnetic fields. As a result, the essential quantitative characteristics of the relaxation process, in particular, the energy barriers of magnetization reversal and the times of the fastest relaxation, cannot be determined. The indicated features of the magnetic relaxation are apparently due to the the presence of apical ligands together with the strong distortion of the equatorial symmetry of CE of Yb^{3+}.

ACKNOWLEDGMENTS

Studies were carried out using the equipment of the JRC PMR IGIC RAS.

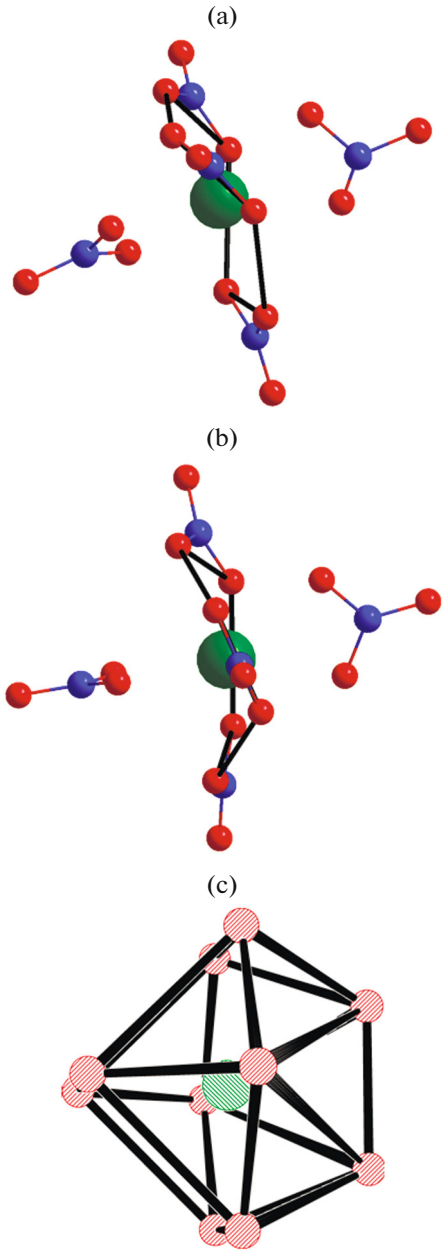

Fig. 5. Distortion of equatoriall planes of Yb CE in **I** (a) and **II** (b) structures in comparison with ideal tetradecahedron (c). Equatorial donor centers and connected by lines for clarity. For each disordered NO_3^-, only one position shown.

FUNDING

We thank the Russian Foundation for Basic Research, RFBR (grant no. 19-29-13015), for the financial support of this study (synthesis and study of complexes **I** and **II**). The study of the **II**·MeOH complex, as well as the elemental analysis of the complexes, was carried out within the framework of the state assignment of the IGIC RAS in the field of fundamental scientific research.

CONFLICT OF INTEREST

The authors declare that they have no conflicts of interest.

SUPPLEMENTARY INFORMATION

The online version contains supplementary material available at https://doi.org/10.1134/S1070328422040066.

REFERENCES

1. Efimov, N., Koroteev, P., Gavrikov, A., et al., *Magnetochemistry*, 2016, vol. 2, no. 4, p. 38.
2. Nikolaevskii, S.A., Yambulatov, D.S., Voronina, J., et al., *ChemistrySelect*, 2020, vol. 5, no. 41, p. 12829.
3. Lutsenko, I.A., Kiskin, M.A., Nikolaevskii, S.A., et al., *ChemistrySelect*, 2019, vol. 4, no. 48, p. 14261.
4. Petrosyants, S.P., Ilyukhin, A.B., Efimov, N.N., et al., *Russ. J. Coord. Chem.*, 2018, vol. 44, no. 11, p. 660. https://doi.org/10.1134/S1070328418110064
5. Bazhina, E.S., Aleksandrov, G.G., Kiskin, M.A., et al., *Eur. J. Inorg. Chem.*, 2018, vol. 2018, no. 47, p. 5075.
6. Li, M., Lan, Y., Ako, A.M., et al., *Inorg. Chem.*, 2010, vol. 49, no. 24, p. 11587.
7. Cheng, J.W., Zhang, J., Zheng, S.T., et al., *Chem. A Eur. J.*, 2008, vol. 14, no. 1, p. 88.
8. Zhu, S.D., Hu, J.J., Dong, L., et al., *J. Mater. Chem.*, vol. 8, no. 45, p. 16032.
9. Mamontova, E., Long, J., Ferreira, R., et al., *Magnetochemistry*, 2016, vol. 2, no. 4, p. 41.
10. Dey, A., Kalita, P., and Chandrasekhar, V., *ACS Omega*, 2018, vol. 3, no. 8, p. 9462.
11. Feltham, H.L.C. and Brooker, S., *Coord. Chem. Rev.*, 2014, vol. 276, p. 1.
12. Mannini, M., Pineider, F., Sainctavit, P., et al., *Nat. Mater.*, 2009, vol. 8, no. 3, p. 194.
13. Baldoví, J.J., Cardona-Serra, S., Clemente-Juan, J.M., et al., *Inorg. Chem.*, 2012, vol. 51, no. 22, p. 12565.
14. Bogani, L. and Wernsdorfer, W., in *Nanoscience and Technology. A Collection of Reviews from Nature J.*, Rodgers, P., Ed., London; Singapore, 2009, p. 194. https://doi.org/10.1142/9789814287005_0020
15. Sanvito, S., *Chem. Soc. Rev.*, 2011, vol. 40, no. 6, p. 3336.
16. Lehmann, J., Gaita-Ariño, A., Coronado, E., et al., *J. Mater. Chem.*, 2009, vol. 19, no. 12, p. 1672.
17. Liu, K., Shi, W., and Cheng, P., *Coord. Chem. Rev.*, 2015, vols. 289–290, no. 1, p. 74.
18. Rinehart, J.D., Fang, M., Evans, W.J., et al., *Nat. Chem.*, 2011, vol. 3, no. 7, p. 538.
19. Liu, C.M., Zhang, D.Q., Su, J.B., et al., *Inorg. Chem.*, 2018, vol. 57, no. 17, p. 11077.
20. Zhang, J.W., Ren, Y.N., Li, J.X., et al., *Eur. J. Inorg. Chem.*, 2018, vol. 2018, no. 9, p. 1099.
21. Yamaguchi, T., Costes, J.P., Kishima, Y., et al., *Inorg. Chem.*, vol. 49, no. 20, p. 9125.
22. Kajiwara, T., Nakano, M., Takahashi, K., et al., *Chem. A Eur. J.*, 2011, vol. 17, no. 1, p. 196.

23. Liu, C.-M., Zhang, D.-Q., Hao, X., et al., *Inorg. Chem. Front.*, 2020, vol. 7, no. 18, p. 3340.
24. Bhanja, A., Schulze, M., Herchel, R., et al., *Inorg. Chem.*, 2020, vol. 59, no. 24, p. 17929.
25. Langley, S.K., Le, C., Ungur, L., et al., *Inorg. Chem.*, 2015, vol. 54, no. 7, p. 3631.
26. Nayak, S., Novitchi, G., Hołyńska, M., et al., *Eur. J. Inorg. Chem.*, 2014, no. 19, p. 3065.
27. Benelli, C. and Gatteschi, D., *Chem. Rev.*, 2002, vol. 102, no. 6, p. 2369.
28. *APEX2 and SAINT*, Madison: Bruker AXS Inc., 2007.
29. Sheldrick, G.M., *SADABS. Program for Scanning and Correction of Area Detection Data*, Göttingen: Univ. of Göttingen, 1997.
30. Sheldrick, G.M., *Acta Crystallogr., Sect. C: Struct. Chem.*, 2015, vol. 71, no. 1, p. 3.
31. Gavrikov, A.V., Ilyukhin, A.B., Belova, E.V., et al., *Ceram. Int.*, 2020, vol. 46, no. 9, p. 13014.
32. Shan, C.Y., Zhao, W.X., Tao, Z., et al., *Inorg. Chem. Commun.*, 2016, vol. 71, p. 109.
33. Evans, D.J., Junk, P.C., and Smith, M.K., *New J. Chem.*, 2002, vol. 26, no. 8, p. 1043.
34. Lipstman, S. and Goldberg, I., *Cryst. Growth Des.*, 2010, vol. 10, no. 4, p. 1823.
35. Truter, M.R., Parsons, D.G., Hughes, D.L., et al., *Inorg. Chim. Acta*, 1985, vol. 110, no. 3, p. 215.
36. Shannon, R.D., *Acta Crystallogr., Sect. A: Cryst. Phys., Diffr., Theor. Gen. Crystallogr.*, 1976, vol. 32, no. 5, p. 751.
37. Llunell, M., Casanova, D., Cirera, J., et al., *SHAPE. Version 2.1*, Barcelona: Universitat de Barcelona, 2013.
38. Kepert, D.L., *Inorganic Sterochemistry*, Berlin-Heidelberg: Springer-Verlag, 1982.
39. Kahn, O., *Molecular Magnetism*, New York: Wiley, 1993.
40. Zhang, J.W., Liu, W.H., Wang, C.R., et al., *ChemistrySelect*, 2019, vol. 4, no. 42, p. 12418.
41. Feltham, H.L.C., Dhers, S., Rouzières, M., et al., *Inorg. Chem. Front.*, 2015, vol. 2, p. 982.
42. Pasatoiu, T.D., Sutter, J.P., Madalan, A.M., et al., *Inorg. Chem.*, 2011, vol. 50, no. 13, p. 5890.
43. Lefeuvre, B., Mattei, C.A., Gonzalez, J.F., et al., *Chem. A Eur. J.*, 2021, vol. 27, no. 26, p. 7362.
44. Petrosyants, S.P., Babeshkin, K.A., Ilyukhin, A.B., et al., *Russ. J. Coord. Chem.*, 2021, vol. 47, no. 4, p. 244. https://doi.org/10.31857/S0132344X2104006X
45. Mondal, A. and Konar, S., *Chem. A Eur. J.*, 2021, vol. 27, no. 10, p. 3449.
46. Petrosyants, S.P., Babeshkin, K.A., Gavrikov, A.V., et al., *Dalton Trans.*, 2019, vol. 48, no. 33, p. 12644.
47. Belio Castro, A., Jung, J., Golhen, S., et al., *Magnetochemistry*, 2016, vol. 2, no. 2, p. 26.
48. Soussi, K., Jung, J., Pointillart, F., et al., *Inorg. Chem. Front.*, 2015, vol. 2, no. 12, p. 1105.
49. Pointillart, F., Jung, J., Berraud-Pache, R., et al., *Inorg. Chem.*, 2015, vol. 54, no. 11, p. 5384.
50. North, J.M., Van De Burgt, L.J., and Dalal, N.S., *Solid State Commun.*, 2002, vol. 123, nos. 1–2, p. 75.
51. Mayans, J., Saez, Q., Font-Bardia, M., et al., *Dalton Trans.*, 2019, vol. 48, p. 641.
52. Rinehart, J. and Long, J., *Chem. Sci.*, 2011, vol. 2, p. 2078.
53. Sugita, M., Ishikawa, N., Ishikawa, T., et al., *Inorg. Chem.*, 2006, vol. 45, no. 3, p. 1299.